

Some electrical characteristics of $\text{Li}_{0.5}\text{Cr}_x\text{Fe}_{2.25-x}\text{O}_4$ spinel structures

A. Sellai*, H.M. Widatallah

Physics Department, Sultan Qaboos University, P.O. Box 36, 123 Al-Khod, Oman

Received 11 November 2003; received in revised form 2 December 2003; accepted 22 December 2003

Available online 6 May 2004

Abstract

Some of the electrical properties of chromium-substituted spinel $\text{Li}_{0.5}\text{Cr}_x\text{Fe}_{2.25-x}\text{O}_4$ with $0.15 \leq x \leq 1.85$, synthesized at 1200°C for 12 h, are examined through impedance measurements and analysis. The electrical resistivity, relaxation frequencies and dielectric constant of $\text{Li}_{0.5}\text{Cr}_x\text{Fe}_{2.25-x}\text{O}_4$ have been investigated versus the composition x . The behavior of these can be satisfactorily described by a hopping mechanism of charge carriers between Fe^{2+} and Fe^{3+} ions on octahedral sites of the spinel lattice.

© 2004 Elsevier Ltd and Techna Group S.r.l. All rights reserved.

Keywords: Spinel structures; Impedance analysis; Lithium ferrites

1. Introduction

Lithium and metal-substituted lithium ferrites are of considerable interest for their potential technological applications as, for example, cathode materials in lithium ion batteries [1,2] and microwave frequency applications [3,4]. The study of electrical conductivity in these materials is important since the associated physical properties like piezoelectricity, pyroelectricity and thermoelectricity are dependent on the nature and the magnitude of conductivity in these materials.

Impedance measurements are routinely used to characterize the dielectric behavior of materials and have proved to be a particularly powerful tool for depicting the electrical conductivity of ionic, electronic, or mixed ceramic materials. Using impedance analysis, it has been possible to resolve, in the frequency domain, the contributions and relative importance to electrical conduction and/or polarization of different phenomena taking place in the sample under study. The response of the sample is usually manifest as capacitive and resistive behaviors attributed predominantly to the bulk grains, the grain boundaries or the defects present at sample–electrode interface.

The ac impedance response of a material can be modeled by a number of R – C parallel cells, each cell representing

the contribution to the overall response of a possibly present phenomenon. The impedance (Z) associated with a single R – C cell is

$$Z = Z_R - jZ_X = \frac{R}{1 + jRC\omega} = \frac{R}{1 + (RC\omega)^2} - j \frac{RC\omega}{1 + (RC\omega)^2} \quad (1)$$

resulting in the relation $Z_X^2 + (Z_R - R/2)^2 = (R/2)^2$, which is the equation of a circle. Similarly, using the electric modulus $M = j\omega C_0 Z$, one obtains

$$M = M_R + jM_X = \frac{-RC_0\omega(RC\omega)}{1 + (RC\omega)^2} + j \frac{RC_0\omega}{1 + (RC\omega)^2} \quad (2)$$

which also leads to the equation of a circle $M_X^2 + (M_R - C_0/2C)^2 = (C_0/2C)^2$, where C_0 is the capacitance of the empty cell.

The electrical data is routinely presented under forms that can be exploited to get useful information from samples under study such as the complex impedance form (Z_X versus Z_R) or loss spectra (ϵ , M or Z versus frequency). These are related to each other by the equations

$$M = j\omega C_0 Z \quad (3)$$

$$\epsilon = \frac{1}{M} = \epsilon_R + i\epsilon_X \quad (4)$$

$$Y = \frac{1}{Z} = j\omega C_0 \epsilon \quad (5)$$

* Corresponding author. Tel.: +968-515-486; fax: +968-514-228.

E-mail address: asellai@squ.edu.om (A. Sellai).

$$\sigma = Y_R \frac{t}{A} \quad (6)$$

where t and A are the thickness and area of the sample, respectively.

The plots in the Z plane are dominated by the resistance element while the plots in the M plane (M_X versus M_R) are dominated by the capacitance. When relative contributions from bulk and grain boundaries are comparable, two semicircular plots appear in both Z and M planes. One single semicircular plot, however, might indicate the dominance of one phenomenon. Bulk responses are generally characterized by a low capacitance (in the pF-range) while grain boundaries give rise to larger (nF-range) capacitances.

We report in this work the impedance data and analysis related to a $\text{Li}_{0.5}\text{Cr}_x\text{Fe}_{2.25-x}\text{O}_4$ spinel structure prepared using conventional ceramic methods. The electric modulus (M) and impedance (Z) plots in the complex plane are employed to study the dielectric behavior of the sample at room

temperature and for different fractional Cr contents (x). The dependence of the ac resistivity and the dielectric constant on x are reported and explained on the basis of hopping between trivalent and divalent Fe ions.

2. Experimental

Cr-substituted spinel lithium ferrite of the composition $\text{Li}_{0.5}\text{Cr}_x\text{Fe}_{2.25-x}\text{O}_4$ ($0.15 \leq x \leq 1.85$) were prepared with the conventional double sintering ceramic technique using high purity reagents Cr_2O_3 , $\alpha\text{-Fe}_2\text{O}_3$, and Li_2CO_3 . The pre-sintering of the samples was carried at 1000°C (12 h) and the final sintering at 1200°C (12 h). X-ray powder diffraction (XRD) analysis has shown all samples to be single-phased. Rietveld refinement of the XRD data gave results that are consistent with those of similar studies for $\text{Li}_{0.5}\text{Cr}_x\text{Fe}_{2.25-x}\text{O}_4$ [5]. The lattice parameters were found to slightly decrease with increasing Cr^{3+} substitution. This unit cell size variation could be attributed to the

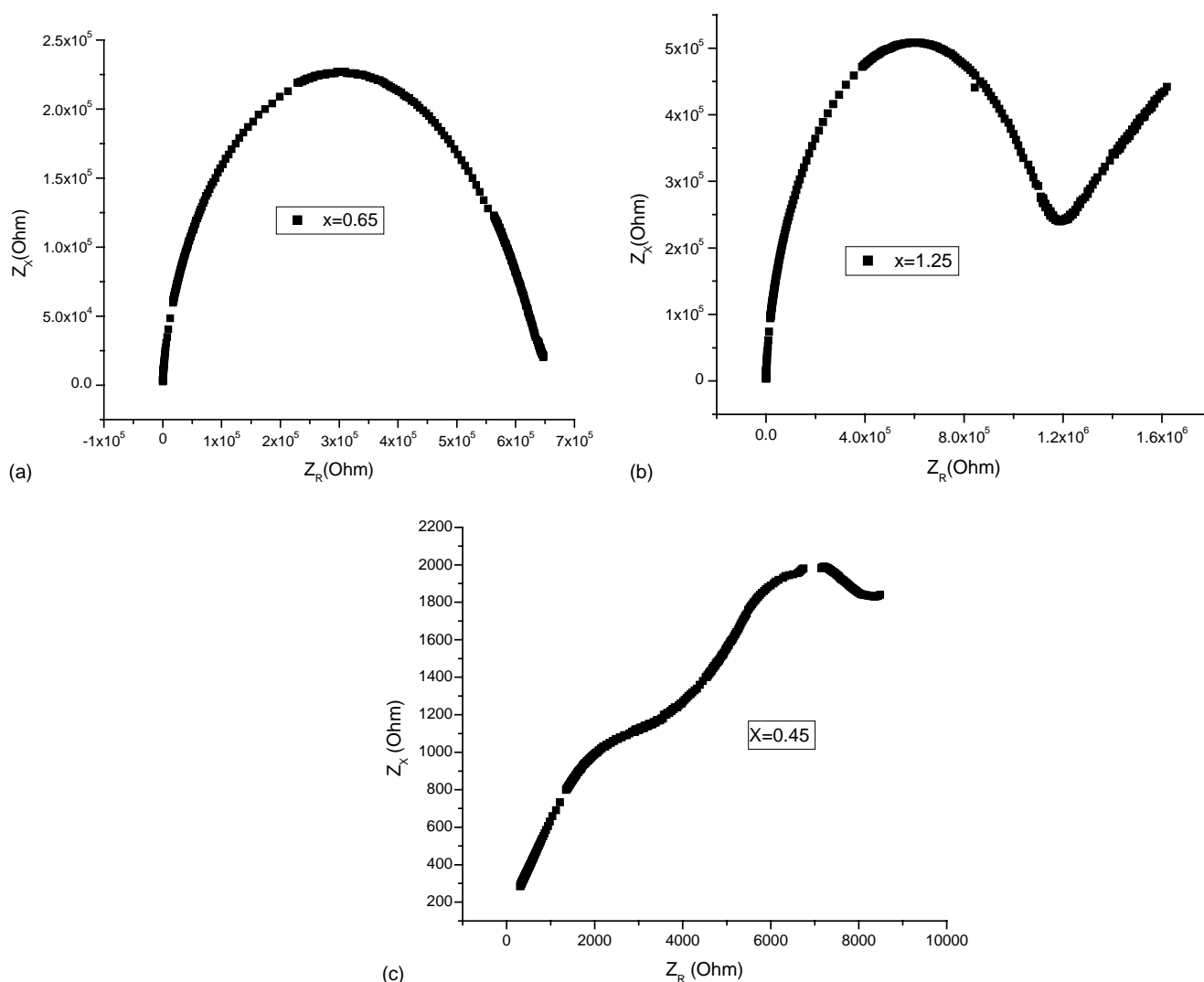


Fig. 1. Impedance (Z_X – Z_R) plots for three different Cr contents (a) $x = 0.65$, (b) $x = 1.25$, and (c) $x = 0.45$.

ionic radius of six-fold-coordinated Cr^{3+} (75.5 pm) being smaller than that of six-fold-coordinated Fe^{3+} (78.5 pm) [6]. Cr^{3+} ions preferentially replace Fe^{3+} ones at octahedral sites due to favorable crystal field effects [5]. According to our preliminary structural analysis, it appears that the cationic distribution in our samples is similar to that given in [5], namely $(\text{Fe})[\text{Li}_{0.5}\text{Cr}_x\text{Fe}_{1.5-x}]\text{O}_4$ for $0 \leq x \leq 1.5$, $(\text{Li}_{0.25}\text{Fe}_{0.75})[\text{Li}_{0.25}\text{Cr}_{1.75}]\text{O}_4$ for $x = 1.75$, and $(\text{Li}_{0.35}\text{Fe}_{0.75})[\text{Li}_{0.15}\text{Cr}_{1.85}]\text{O}_4$ for $x = 1.85$ where round brackets denote tetrahedral sites and square brackets denote octahedral ones.

In order to carry out the two-terminal impedance measurements using the Impedance Analysers HP-4192 and HP-4285A, pellets were cut into small pieces of regular shapes then silver paint and gold-plated contact probes were used to make electrical contacts on both sides of the pellets. Prior to measurements, the impedance, capacitance and resistance of the empty cell were measured over the entire frequency range considered (50 Hz to 30 MHz) so that they are automatically subtracted from subsequently measured data.

To obtain the dielectric functions from capacitance and D -loss measurements, first the capacitance C_s^m of the sample was measured over the entire frequency range. The measured C_s^m includes C_s of the sample and that of connecting wires C_{wires} : $C_s^m = C_s + C_{\text{wires}}$. The capacitance C_{air} of the empty cell was similarly measured $C_{\text{air}}^m = C_{\text{air}} + C_{\text{wires}}$, as well as the capacitance (C_k) of a known material $C_k^m = C_k + C_{\text{wires}}$. Knowing that $C_i = \epsilon_i A/t$ we can deduce

$$C_{\text{wires}} = \frac{C_k C_{\text{air}}^m - C_k^m}{C_k - 1} \quad (7)$$

and

$$\epsilon_R = \frac{C_s^m - C_{\text{wires}}}{C_{\text{air}}^m - C_{\text{wires}}}, \quad \epsilon_X = \epsilon_R \tan \delta \quad (8)$$

where $\tan \delta$ is the measured D -loss.

3. Results and discussion

Depending on the amount of the substituted Cr, the obtained Z_X – Z_R plots are of three types. Nearly perfect semicircles (Fig. 1a) are obtained for Cr contents corresponding to $x = 0.65$, 0.95 and 1.15 revealing that the response originated from a single R – C element associated with the bulk of the sample. The low capacitance values derived in this case, of the order of pF, are typical of a bulk response. For higher Cr contents ($x \geq 1.25$) the plots (Fig. 1b) are semicircles at high frequencies followed by what appears to be an arc of a second semicircle that is severely depressed implying a non-homogeneous electrical behavior of grains. This, we could not investigate further due to the frequency limitations of the equipment. For lower Cr contents ($x \leq 0.45$), the shape of the curves observed (Fig. 1c) could be due to the overlapping of two or more arcs of semicircles, an indication of a non-dominant single contribution. The overlapping semicircles, at high and low frequencies, could in fact be attributed to charge transport within the grain interior and grain boundary effects. The high capacitance values, of the order of nF, are in fact, typical of a grain boundary response. Similar behavior was also shown by the (not shown here) M_X – M_R plots.

The values of R and C are derived from both the Z -plots, dominated by the resistive part, and the M -plots more

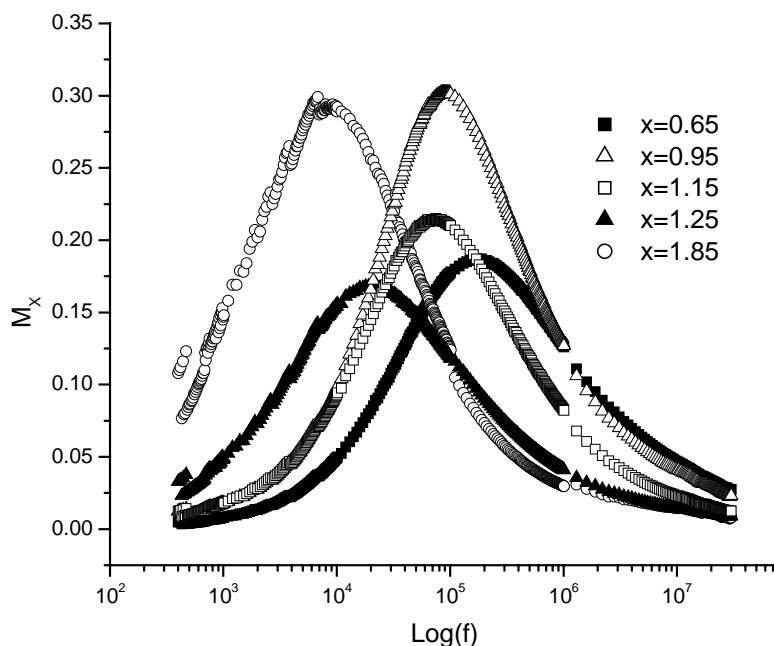


Fig. 2. Imaginary part of electrical modulus (M_X) vs. $\log f$ for different Cr contents (x).

sensitive to the capacitive behavior. The second intercept on the real axis in the Z_X-Z_R (M_X-M_R) plot corresponds to the resistance (capacitance) due to bulk grain behavior. An increase in x shifts the intercept towards higher values indicating an increase in the resistance. The extracted capacitances, however, fall in two regions: a pF region, typical of bulk response, for $x \geq 0.65$ and a nF region, typical of grain boundary response, for $x \leq 0.45$.

The relaxation frequency is an intrinsic characteristic property that can be used to yield information on the dielectric behavior of the material. Through the imaginary part of the electric modulus (M_X), directly related to the dielectric

loss (Eq. (3) above), relaxation frequencies can be obtained. The maximum in M_X is a normal behavior observed by several authors [7–9] and it is believed to be due to the hopping of electrons between Fe^{2+} and Fe^{3+} sites, which is considered to be responsible for the conduction mechanism in these ferrites [10,11]. When the frequency of the externally applied ac signal matches the hopping frequency, a maximum loss might result leading to a maximum in M_X . Fig. 2 shows M_X versus log-frequency plots with peak positions shifting to higher frequency as x is decreased. Relaxation frequencies obtained from these plots are given in Table 1 for all the values of x , except for $x \leq 0.45$ where

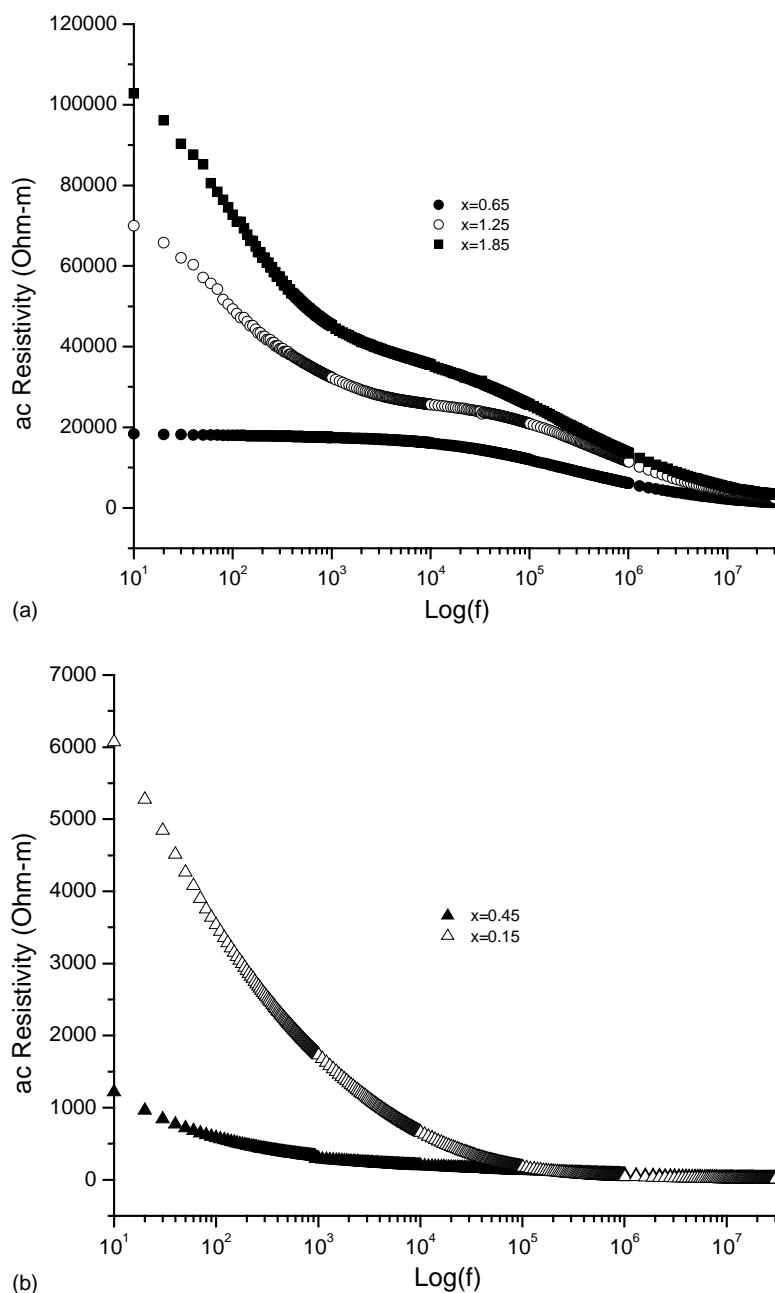


Fig. 3. (a and b) Variations of ac resistivity with the frequency for different Cr contents (x).

Table 1
Relaxation frequency for various Cr content (x)

x (Cr)	f_{Peak} (kHz)
0.65	180
0.95	92
1.15	75
1.25	19
1.85	6.8

the peaks happen to be outside the frequency range considered. These results suggest a decrease in the relaxation times as the fraction of Cr is decreased.

Furthermore, from Fig. 3a and b, the ac resistivity (ρ_{ac}) in all samples decreases as the frequency increases and tends to a constant value at high frequencies, beyond 1 MHz in general. On the other hand, the ac resistivity drops monolithically as x decreases from 1.85 to 0.15. We believe that this behavior could be explained by electron hopping which involves exchange of electrons between ions of the same element present in different valence states, and distributed randomly over crystallographically equivalent lattice sites. In the inverse-spinel $\text{Li}_{0.5}\text{Fe}_{2.25}\text{O}_4$, it is known that all Li^+ ions and most of the Fe^{3+} ions are randomly distributed over the octahedral sites while the tetrahedral sites are occupied by the remaining Fe^{3+} , with the oxygen ions in the octahedral sites forming a cubic array in the structure [12]. A high concentration of Fe^{2+} is usually seen as responsible for a low resistivity in the material. Fe^{2+} ions could originate from the conversion of a small amount of Fe^{3+} ions during the sintering process at very high temperatures. Ideally, in $\text{Li}_{0.5}\text{Fe}_{2.5}\text{O}_4$ all iron ions are Fe^{3+} . However, the high sintering temperatures (1000–1200 °C) for prolonged times (12 h),

as used in the preparing the Cr-substituted $\text{Li}_{0.5}\text{Fe}_{2.5}\text{O}_4$ samples studied here, result in the volatility of Li_2O [4,13] leading, in turn, to reduction of some Fe^{3+} to Fe^{2+} . This has been explained in detail in Ref. [13] and here we only briefly discuss it. When Li^+ is removed from a region in the crystal (e.g. a selected unit cell in the bulk) and assuming that unit cell retains its full complement of 32 O^{2-} ions, the positive charge of the departed Li^+ must be compensated. This is accomplished by diffusion of Fe^{3+} from the surface as the O^{2-} on the surface is removed. Each vacated Li^+ site is re-occupied, in effect, by an Fe ion diffusing from the surface. However, charge neutrality is maintained by the concurrent reduction of that ion from Fe^{3+} to Fe^{2+} . The composition of the non-substituted lithium ferrite can now be represented as $\text{Li}_{0.5-y}\text{Fe}^{2+}_{2y}\text{Fe}^{3+}_{2.5-y}\text{O}_4$. The same can be assumed to take place for the present Cr-substituted $\text{Li}_{0.5}\text{Fe}_{2.5}\text{O}_4$.

Therefore, a partial substitution of the Fe^{3+} on either the octahedral or tetrahedral site by other ions is expected to result in a change in both the magnetic and conduction properties of the compound. Since the increase in conductivity is related to electron exchange between divalent and trivalent Fe ions, the gradual substitution of Fe^{3+} (increasing x) by Cr might result in less Fe^{3+} ions available for the hopping mechanism leading to a decrease in conductivity (increase in ρ_{ac}). The tendency towards a constant resistivity at higher frequencies is also a consequence of hopping carriers no longer able to follow beyond a certain frequency, the changes imposed by the externally applied ac signal.

A strong correlation is believed to exist between the conduction mechanism and the dielectric behavior of ferrites [10,14]. Fig. 4 is a plot of ϵ_R , obtained following Eq. (8), versus $\log f$ for $x = 0.15, 0.45, 0.65, 1.25$. It shows that ϵ_R increases as x decreases which is the opposite behavior

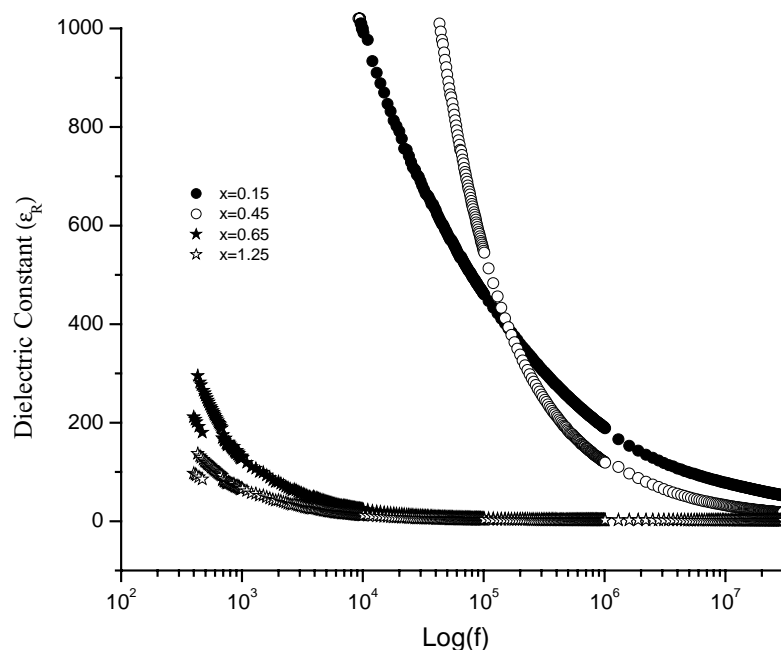


Fig. 4. Dielectric constant (ϵ_R) vs. $\log f$ for different Cr contents (x).

of ρ_{ac} . Knowing that electron exchange between Fe^{3+} and Fe^{2+} also results in local displacements affecting directly the polarization of the ferrite. Lower $\text{Fe}^{3+} \leftrightarrow \text{Fe}^{2+}$ exchanges due to a lack of substituted Fe^{3+} should lead to the least possible polarizations, which can explain the variations of ε_R with x .

In conclusion, impedance measurements and analysis performed on $\text{Li}_{0.5}\text{Cr}_x\text{Fe}_{2.25-x}\text{O}_4$ ferrites reveal a response that is dominated by a grain boundary behavior for $x \leq 0.45$ and by the bulk of the material otherwise. The variations of the relaxation frequency, the increase in ac resistivity and the behavior of the dielectric constant, as the Cr content is increased, were ascribed to a hopping mechanism between Fe^{3+} and Fe^{2+} ions and the availability of ferrous ions on octahedral sites.

References

- [1] M.N. Obrovac, O. Mao, J.R. Dahn, *Solid State Ionics* 112 (1998) 9.
- [2] Y. Sakurai, H. Arai, J. Yamaki, *Solid State Ionics* 113–115 (1998) 29.
- [3] J. R. Dahn, U. Vom Sacken, C.A. Michal, *Solid State Ionics* 44 (1990) 87.
- [4] G. M. Argentina, P.D. Baba, *IEEE Trans. Microwave Theory Tech.* MTT-22 (1974) 652.
- [5] M.V. Kuznetsov, Q.A. Pankhurst, I.P. Parkin, *J. Phys. D: Appl. Phys.* 31 (1998) 2886.
- [6] M. Winter, <http://www.webelement.com>, The University of Sheffield and WebElements Ltd., UK.
- [7] R. Laishram, S. Phanjoubam, H.N.K. Sarma, C. Prakash, *J. Phys. D: Appl. Phys.* 32 (1999) 2151.
- [8] N.V. Prasad, G. Prasad, T. Bhimasankaram, S.V. Suryanarayana, G.S. Kumar, *Bull. Mater. Sci.* 24 (5) (2001) 487.
- [9] M. Hartmanova, F. Kundracik, J. Schneider, T.V. Oreshnikova, *Acta Physica Slovaca* 49 (3) (1999) 419.
- [10] K.V. Kumar, A.C.S. Reddy, D. Ravinder, *J. Magn. Magn. Mater.* 263 (1–2) (2003) 121.
- [11] N. Rezlescu, E. Rezlescu, *Phys. Stat. Sol.* A23 (1974) 575.
- [12] H.M. Widadallah, C. Johnson, F. Berry, M. Pekala, *Solid State Commun.* 120 (2001) 171.
- [13] D.H. Ridgley, H. Lessoff, J.D. Childress, *J. Am. Ceram. Soc.* 53 (1970) 304.
- [14] K. Iwachi, *Jpn. J. Appl. Phys.* 10 (1971) 1520.